Journal of Materials Chemistry A

Accepted Manuscript

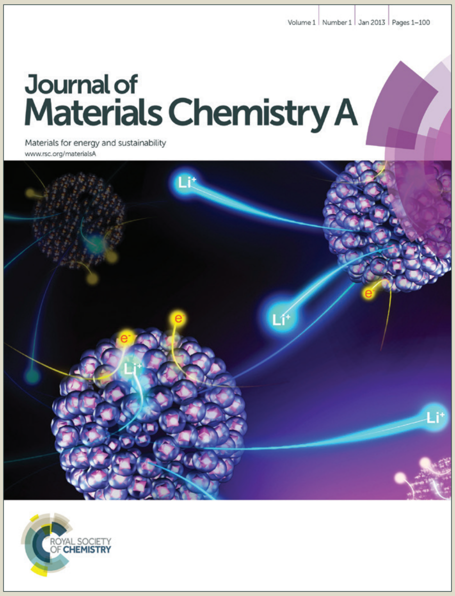

ROYAL SOCIETY OF CHEMISTRY

www.rsc.org/materialsA

Journal of Materials Chemical A RSCPublishing

COMMUNICATION

Hierarchical Ru Nanospheres as Highly Effective Cathode Catalysts for Li-O_2 Batteries

Cite this: DOI: 10.1039/x0xx00000x

D.W. Su,*[a] S. X. Dou[b] and G. X. Wang*[a,c]

Received 00th January 2012,
Accepted 00th January 2012

DOI: 10.1039/x0xx00000x

www.rsc.org/

Carbon-free, hierarchical Ru nanospheres are reported as an effective cathode catalyst for the Li-O_2 battery. The hierarchical Ru nanospheres were syntheized by a simple one-step hydrothermal method. As evaluated by electrochemical measurements, it was found that the carbon-free hierarchical Ru nanosphere cathode can significantly reduce discharge and charge overpotential (~ 0.3 V with the capacity limited to 1000 mA h g^{-1}) with a high discharge capacity of 3445 mA h g^{-1} at current density of 200 mA g^{-1} (ORR). This superior oxygen evolution reaction (OER) and oxygen reduction reaction catalytic performance can be maintained over long time cycling at different current densities. *Ex-situ* scanning electron microscopy, X-ray diffraction, and Raman measurements reveal that leaf-shaped Li_2O_2 is the only reaction product during the discharge process, and the hierarchical Ru nanospheres can effectively decompose the Li_2O_2 discharge product, facilitate the OER, and promote a high round-trip efficiency. Therefore, the carbon-free hierarchical Ru nanospheres are a promising cathode catalyst for rechargeable Li-O_2 batteries with low charge overpotential, long cycle life, and high specific capacity.

1 Introduction

Because of their high theoretical energy density (3505 Wh kg^{-1}),[1-4] Li-O_2 batteries have been considered to be one of the most promising systems as future power sources for electric vehicles. Practical Li-O_2 batteries are still suffering from several serious problems, such as high overpotential, low round-trip efficiency and low energy density.[5-9] Many studies are now focusing on cathode catalysts, in order to improve the oxygen evolution reaction (OER) and oxygen reduction reaction (ORR) for Li-O_2 batteries. In these studies, carbon-based materials are the main candidates for the rechargeable Li-O_2 batteries.[10-15] It has been reported, however, that carbon will be directly involved in the charge and discharge reactions, generating by-products, which are not dissolved in the electrolyte and accumulate in the cathode electrode, covering the active materials.[16-18] This could block the oxygen diffusion pathways and thus the reaction between Li ions and oxygen, and also cause volume expansion of the electrode, resulting in its degradation. Therefore, finding carbon-free cathode materials is becoming the crucial factor for Li-O_2 batteries.

Some alternative catalyst materials have been identified as effective cathodes for Li-O_2 batteries, including nanocrystalline mixed metal oxides with an expanded pyrochlore structure,[19] noble metals,[1] Fe/N/C composites,[20] and indium tin oxide (ITO),[4]. Nevertheless, these catalysts still have problems, such as high overpotential between charge and discharge, poor cycling stability, low Coulombic efficiency, and low rate capability.[5-8] Therefore, identifying suitable carbon-free cathode catalysts is still the current main challenge. Recently, ruthenium (Ru) has been verified to be a good catalyst for the OER in Li-O_2 batteries.[21-23] When Ru was combined with carbon materials as cathode catalysts, the overpotential between the charge and discharge processes was greatly decreased, which shows its unique catalytic performance for Li-O_2 batteries. It was reported that when ruthenium nanocrystals supported on carbon black or porous graphene, the electrodes showed an excellent catalytic activity for ORR/OER with a high reversible capacity and low charge-discharge over-potential.[24, 25] Zhou *et al*. reported Ru nanoparticles supported on Sb-doped TiO_2 particles also demonstrated low overpotentials and high capacity.[26] Later, they studied the RuO_2 hollow spheres cathode, which can obtain 1400 mA h g^{-1} capacity.[27]

So far, there has been no research on pure Ru cathode catalyst for Li-O_2 batteries. Herein, we report the synthesis of Ru nanocrystals as highly effective cathode catalysts for Li-O_2 batteries. The as-prepared Ru nanocrystals present hierarchical nanosphere morphology. After characterization by electrochemical measurements, it was revealed that the hierarchical Ru nanospheres significantly reduce the discharge and charge overpotential (~ 0.3 V at capacity limited to 1000 mA h g^{-1}) and achieved the high discharge capacity of 3445 mA h g^{-1} at current density of 200 mA g^{-1}. These superior OER and ORR catalytic properties can be maintained for many cycles at different current densities, indicating the stability of the hierarchical Ru nanospheres. We further conducted *ex-situ* X-ray diffraction (XRD), Raman, and scanning electron microscopy (SEM) measurements to investigate the reaction products. It was found that only leaf-shaped Li_2O_2 was generated during the discharge process and that the Li_2O_2 could be completely decomposed during the charge process. Therefore, the hierarchical Ru nanospheres are a promising cathode catalyst for rechargeable Li−O_2 batteries with low charge overpotential, long cycle life, and high specific capacity.

2 Experimental Section

2.1 Synthesis and Method.

The hierarchical Ru nanospheres were synthesized by a simple one-step hydrothermal method. In a typical process, 20 mL $RuCl_3 \cdot nH_2O$ (2mg mL^{-1}, Sigma-Aldrich, ≥ 98 %) solution was added to 20 mL 10 M NaOH (Sigma-Aldrich, ≥ 99 %) solution. After stirring vigorously for 3 hours, the mixed solution was loaded into a Teflon vessel (90 mL in capacity). The Teflon vessel was sealed and inserted into a protective stainless steel autoclave. Then, it was heated up to 200 ˚C and maintained at this temperature for 12 h. After the reaction was completed, the suspension was filtered, and the precipitate was washed several times with distilled water and ethanol. The final product was collected after being dried in a vacuum oven overnight at 80 ˚C.

2.2. Structural and physical characterization.

The crystal structure and phase of the materials were characterized by X-ray diffraction (XRD, Siemens D5000) using Cu K_α radiation. The morphology was analyzed by field emission scanning electron microscopy (FESEM, Zeiss Supra 55VP). The details of the structure were further characterized by transmission electron microscopy (TEM) and high-resolution TEM (HRTEM, JEOL JEM-2011). Selected area electron diffraction (SAED) patterns were recorded by a Gatan charge-coupled device (CCD) camera in a digital format. Atom-resolved HRTEM images were obtained by high-angle annular dark field scanning TEM (HAADF-STEM, JEOL JEM-ARM200F). The optical images were collected with a Canon EOS 660D camera. Raman spectra were collected using a Renishaw inVia Raman spectrometer system (Gloucestershire, UK) equipped with a Leica DMLB microscope (Wetzlar, Germany) and a 17 mW at 633 nm Renishaw helium neon laser source.

2.3. Electrochemical testing.

Swagelok-type cells were designed to investigate the charge and discharge properties and the cyclability in Li-O_2 batteries, which consisted of a stainless steel cylinder plunger to support a Li foil anode (3 mm × ø 15 mm) and a special stainless steel tube to allow oxygen access to the back side of the cathode. The electrodes were prepared as follows: Catalyst slurry was prepared by mixing the as-prepared catalysts (80 wt. %) with poly(tetrafluoroethylene) (PTFE) (20 wt. %) in isopropanol. The mixture was then coated on a glass fibre separator. The cathode electrodes were cut into disks with a diameter of 14 mm and dried at 110 °C in a vacuum oven overnight. The typical loading of the air electrode is about 0.8 mg cm^{-2}. The cathode was placed on the separator, and a disk of thin open 316 stainless steel mesh was placed on top to act as a current collector. The entire cell was gas-tight, except for the stainless steel mesh window, which exposed the porous cathode to the O_2 atmosphere. The Li-O_2 cells were assembled in an Ar filled glove box (Unilab, MBRAUN, Germany) with water and oxygen levels less than 0.1 ppm. A glass microfiber filter (Whatman, ø 21 mm) separator was used, soaked in an electrolyte consisting of 1 M $LiNO_3$ (99.99%, Sigma-Aldrich) in dimethyl sulfoxide (DMSO, anhydrous, > 99.9%, Sigma-Aldrich). The water content in the electrolyte is less than 0.1 ppm. All measurements were conducted in 1 atm dry oxygen atmosphere to avoid any negative effects of humidity and CO_2. Galvanostatic discharge-charge testing was conducted on a Neware battery testing system. In order to investigate the charge and discharge products and the corresponding structural and morphological changes, the cells were charged and discharged to the required voltages, and then opened in the glove box. The active materials were removed from the electrodes and washed with DMSO before being used for *ex-situ* XRD, SEM, and Raman analyses.

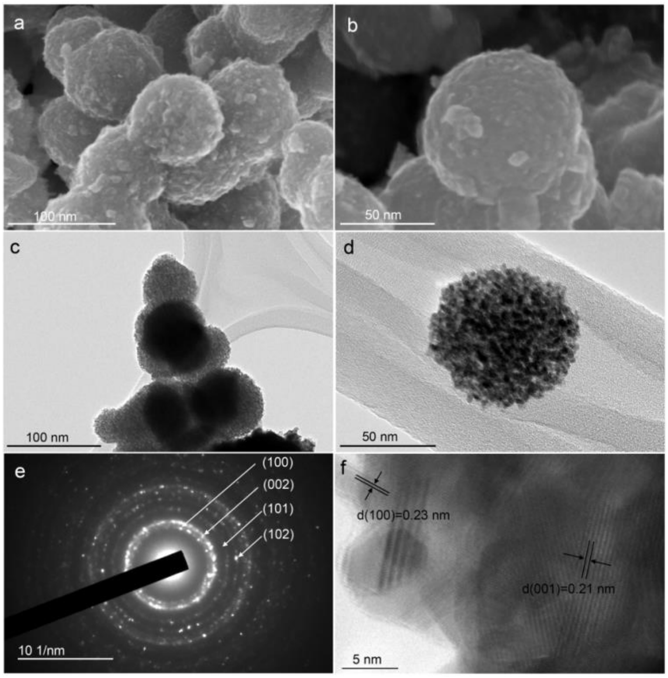

Fig. 1. a, b. FESEM images of hierarchical Ru nanospheres. c. Low magnification TEM image of hierarchical Ru nanospheres. d. High magnification TEM image of hierarchical Ru nanosphere. e. Corresponding selected area electron diffraction pattern. f. Lattice-resolved TEM image of hierarchical Ru nanospheres.

3 Results and discussion

3.1 Phase, morphology and structure characterization

The morphology of the as-prepared Ru nanocrystals was observed by FESEM. The low magnification FESEM images (Fig. S1, Supporting information, SI) show that they have the nanosphere architecture with particle size around 80 nm. From the high magnification FESEM images (Fig. 1a, b), it can be seen that the as-prepared Ru nanospheres consist of primary nanoparticles. Through Rietveld refinement of the XRD pattern, the phase of the Ru nanospheres was further identified (Fig. S2, SI). The XRD pattern can be fully refined as pure hexagonal Ru with satisfied convergence factors (R_{wp} = 9.87 %, R_p = 10.17 %). We conducted TEM and HRTEM observation to further analyze the structure and phase of the Ru nanospheres. The low magnification TEM image in Fig. 1c presents the characteristic features of the nanospheres. The TEM image of a typical free-standing Ru nanosphere (Fig. 1d) clearly demonstrates that it is composed of primary nanocrystal building blocks. The nanocrystals have sizes of less than 10 nm. Fig. 1e is the corresponding selected area electron diffraction (SAED) pattern, which can be fully indexed to pure hexagonal Ru phase. In the lattice-resolved high resolution HRTEM image (Fig. 1f), it can be seen that the primary Ru nanocrystals are around 5 nm in size. The *d*-spacings of 0.23 and 0.21 nm can be clearly identified as the characteristic of the (100) and (001) crystal planes of hexagonal Ru, respectively.

3.2. Electrochemical performance of hierarchical Ru nanospheres for Li-O$_2$ batteries.

The electrocatalytic activities of hierarchical Ru nanospheres as cathode material were investigated by the galvanostatic charge-discharge measurements. Typical charge-discharge voltage profiles are shown in Fig. 2. Hierarchical Ru nanospheres exhibited the high initial discharge capacity of 3445 mA h g^{-1} at current density of 200 mA g^{-1} (Fig. 2a). The corresponding charge capacity can reach up to 3315 mA h g^{-1}. Furthermore, the charge and discharge profiles are obviously different from those of carbon based cathode materials, and very flat curves are presented at 2.76 V and 3.52 V for discharge and charge processes, respectively. This indicates 0.76 V overpotential, which is smaller than that of carbon-based cathode materials for Li-O$_2$ batteries,[15, 28-30] suggesting the superior electrochemical performance of the hierarchical Ru nanospheres. Furthermore, this low overpotential between charge and discharge processes can be maintained for 20 cycles under fully charged and discharged test conditions in the voltage range of 2 – 4 V, indicating the stable electrochemical properties of the hierarchical Ru nanosphere cathode. The discharge capacity of the 2nd cycle was 3358 mA h g^{-1}, and 2861 and 2255 mA h g^{-1} were retained for the 10th and 20th cycles, respectively. When the current density was increased to 400 mA g^{-1}, the overpotential between charge and discharge processes was still only around 0.78 V, and this could be maintained for more than 20 cycles, as shown in Fig. S3 (SI). The discharge capacities of 3023, 2938, 2435, and 1872 mA h g^{-1} were obtained for the 1st, 2nd, 10th, and 20th cycles, respectively. The results indicate that the as-prepared hierarchical Ru nanospheres feature good rate capability.

We also conducted restricted capacity measurements (1000 mA h g^{-1}) to evaluate the electrochemical performance of the Ru nanospheres at various current densities. A low overpotential of 3 V between charge and discharge processes was achieved when the current density was 200 mA g^{-1} (Fig. 2b). This is the lowest value of overpotential reported so far for Li-O$_2$ batteries. This low value is sustainable for 20 cycles with no obvious increase. When the current density was increased to 400 mA g^{-1}, the overpotential was 0.5 V, and there was no increase within 50 cycles (Fig. 2c). Even when the current density was increased to 500 mA g^{-1}, the hierarchical Ru nanosphere electrode still presented a low overpotential of 0.53 V (Fig. 2d) for 80 cycles. These results indicate that the hierarchical Ru nanosphere electrode has high catalytic activity towards the OER.

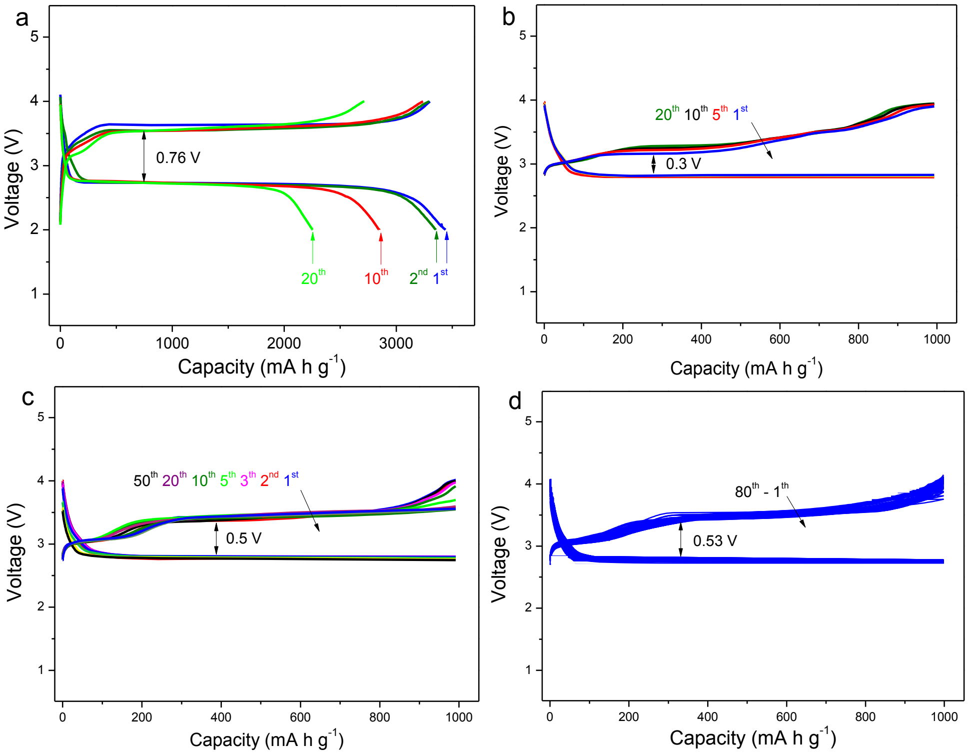

Fig. 2. Charge and discharge profiles for selected cycles of the hierarchical Ru nanosphere electrode: at (a) current density of 200 mA g^{-1}. Charge and discharge profiles with the capacity restricted to 1000 mA h g^{-1} at (b) 200, (c) 400, and (d) 500 mA g^{-1} current densities.

To verify the reaction products, we conducted *ex-situ* XRD, Raman, and SEM measurements. From the *ex-situ* XRD patterns (Fig. 3a) of the discharged hierarchical Ru nanosphere electrode, except for the Ru diffraction peaks, the main peaks can be indexed to Li_2O_2 (JCPDS Card No. 09-0355) with hexagonal symmetry (space group: $P\bar{6}$). When the electrode was fully charged, the peaks corresponding to the Li_2O_2 completely disappeared, suggesting high reversibility of the hierarchical Ru nanosphere electrode for Li-O_2 batteries. The Raman shift at around 787 cm^{-1} in the *ex-situ* Raman spectra (Fig. 3b) further confirm the presence of the discharge product Li_2O_2, and no other by-products were generated during this process.

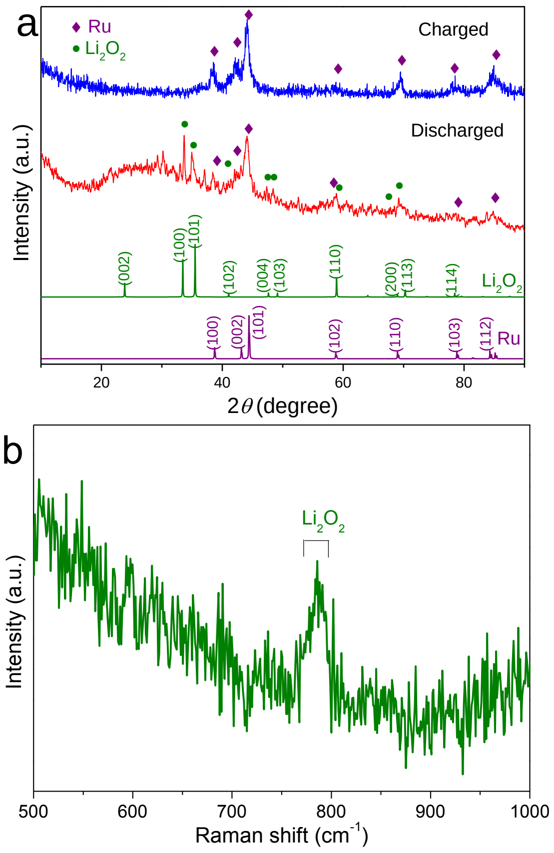

Fig. 3. a. *Ex-situ* XRD patterns of charged and discharged hierarchical Ru nanosphere electrodes. b. *Ex-situ* Raman spectrum of discharged hierarchical Ru nanosphere electrode.

We employed *ex-situ* FESEM characterisation to analyse the morphologies of the hierarchical Ru nanosphere electrode in the fully discharged and charged states. When the electrode was fully discharged, the electrode was fully covered by the reaction product Li_2O_2, as shown in the low magnification *ex-situ* FESEM image in Fig. 4a. Moreover, the Li_2O_2 product presents a leaf-shaped morphology, as shown in the high magnification *ex-situ* FESEM image in Fig. 4b. It is also revealed that the Li_2O_2 has a particle size of ~ 500 nm. The *ex-situ* TEM image (Fig. 4c) of the fully discharged Ru nanospheres electrode further shows the leaf-shaped Li_2O_2 wrinkles. The corresponding SAED pattern of Fig. 4c can be well indexed as crystalline hexagonal Li_2O_2 and Ru as shown in Fig. 4d. When the electrode was fully charged, the discharge product completely disappeared, and the hierarchical Ru nanosphere morphology appeared, as shown in Fig. 4e and f, indicating the high reversibility of the as-prepared hierarchical Ru nanospheres. This is also the main reason why superior OER and ORR catalytic properties were achieved in the Li-O_2 batteries.

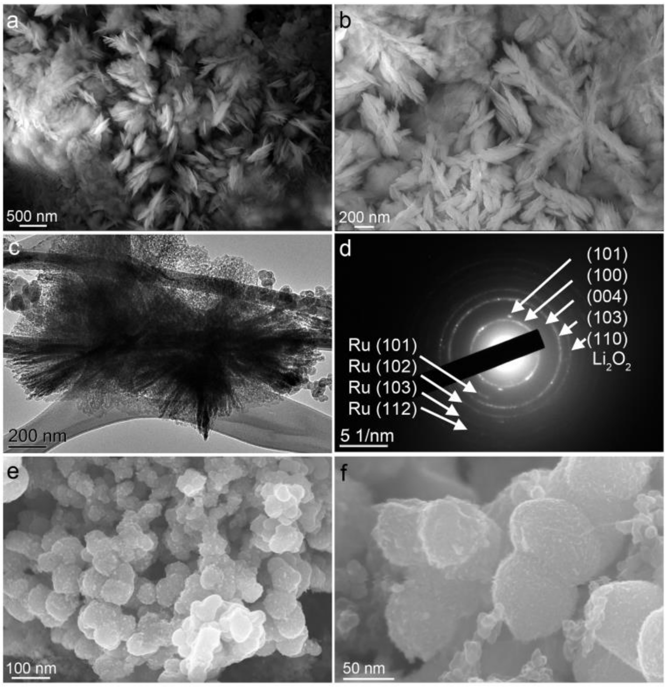

Fig. 4. *Ex-situ* FESEM (a, b) and TEM (c, d) images of fully discharged Ru nanospheres electrode and *Ex-situ* FESEM images of fully charged (e, f) hierarchical Ru nanospheres electrode.

4 Conclusion

Hierarchical Ru nanospheres have been synthesized by a simple hydrothermal method. The electrochemical testing shows that the hierarchical Ru nanospheres can work as an effective cathode catalyst for Li-O_2 batteries. They significantly reduced the discharge and charge overpotential and achieved high specific capacity (3445 mA h g^{-1} at current density of 200 mA g^{-1}) via the effects on the OER. Furthermore, when the hierarchical Ru nanosphere electrode was tested with the capacity limited to 1000 mA h g^{-1}, it demonstrated the low overpotential of ~ 0.3 V at the current density of 200 mA g^{-1}. It also showed superior cycling stability at different current densities and high rate performance. From the *ex-situ* XRD, Raman, and SEM analyses, leaf-shaped Li_2O_2 was identified as the only discharge product, and it was revealed that the Li_2O_2 can be completely decomposed during the charge process, indicating its superior reversibility as cathode catalysts for Li-O_2 batteries. Therefore, the hierarchical Ru nanospheres are promising cathode catalysts for rechargeable Li−O_2 batteries with low charge overpotential, long cycle life, and high specific capacity.

Acknowledgements

This original research was proudly supported by Commonwealth of Australia through the Automotive Australia 2020 Cooperative Research Centre (AutoCRC) and the Fundamental Research Funds for the Central Universities of China (NE2014301). The authors acknowledge the use of facilities within the UOW Electron Microscopy Centre. The authors also would like to thank Dr. Tania Silver for critical reading.

Notes and references

[a] Centre for Clean Energy Technology, Faculty of Science, University of Technology, Sydney, NSW 2007, Australia.. Dawei.Su@uts.edu.au, Guoxiu.Wang@uts.edu.au

[b] Institute for Superconducting and Electronic Materials, University of Wollongong, Wollongong, NSW 2522, Australia.

[c] College of Material Science and Technology, Nanjing University of Aeronautics and Astronautics, Nanjing 210016, P.R. China

Electronic Supplementary Information (ESI) available: Low magnification FESEM images and Rietveld refinement pattern of X-ray diffraction data for hierarchical Ru nanospheres. Charge and discharge profiles for selected cycles of the hierarchical Ru nanosphere electrode at current density of 400 mA g^{-1}. See DOI: 10.1039/b000000x/

1. Z. Peng, S. A. Freunberger, Y. Chen and P. G. Bruce, *Science*, 2012, **337**, 563-566.
2. P. G. Bruce, S. A. Freunberger, L. J. Hardwick and J.-M. Tarascon, *Nat. Mater.*, 2012, **11**, 19-29.
3. M. M. O. Thotiyl, S. A. Freunberger, Z. Peng, Y. Chen, Z. Liu and P. G. Bruce, *Nat. Mater.*, 2013, **12**, 1050–1056.
4. F. Li, D.-M. Tang, Y. Chen, D. Golberg, H. Kitaura, T. Zhang, A. Yamada and H. Zhou, *Nano Lett.*, 2013, **13**, 4702-4707.
5. J. Lu, L. Li, J.-B. Park, Y.-K. Sun, F. Wu and K. Amine, *Chem. Rev.*, 2014, **114**, 5611–5640.
6. G. Zhao, R. Mo, B. Wang, L. Zhang and K. Sun, *Chem. Mater.*, 2014, **26**, 2551-2556.
7. X. Han, F. Cheng, C. Chen, Y. Hu and J. Chen, *Nano Res.*, 2014, 1-9.
8. Q. Li, P. Xu, W. Gao, S. Ma, G. Zhang, R. Cao, J. Cho, H. L. Wang and G. Wu, *Adv. Mater.*, 2014, **26**, 1378-1386.
9. J.-J. Xu, Z.-L. Wang, D. Xu, L.-L. Zhang and X.-B. Zhang, *Nature Commun.*., 2013, **4**.
10. J. Xiao, D. Mei, X. Li, W. Xu, D. Wang, G. L. Graff, W. D. Bennett, Z. Nie, L. V. Saraf and I. A. Aksay, *Nano Lett.*, 2011, **11**, 5071-5078.
11. E. Yoo and H. Zhou, *ACS Nano*, 2011, **5**, 3020-3026.
12. Z. L. Wang, D. Xu, J. J. Xu, L. L. Zhang and X. B. Zhang, *Adv. Funct. Mater.*, 2012, **22**, 3699-3705.
13. T. Zhang and H. Zhou, *Angew. Chem. In. Edit.*, 2012, **51**, 11062-11067.
14. R. R. Mitchell, B. M. Gallant, C. V. Thompson and Y. Shao-Horn, *Energy Environ. Sci.*, 2011, **4**, 2952-2958.
15. H. D. Lim, K. Y. Park, H. Song, E. Y. Jang, H. Gwon, J. Kim, Y. H. Kim, M. D. Lima, R. O. Robles and X. Lepró, *Adv. Mater.*, 2013, **25**, 1348-1352.
16. B. D. McCloskey, A. Speidel, R. Scheffler, D. C. Miller, V. Viswanathan, J. S. Hummelshøj, J. K. Nørskov and A. C. Luntz, *J.Phys. Chem. Lett.*, 2012, **3**, 997-1001.
17. B. D. McCloskey, R. Scheffler, A. Speidel, D. S. Bethune, R. M. Shelby and A. C. Luntz, *J. Am. Chem. Soc.*, 2011, **133**, 18038-18041.
18. B. D. McCloskey, D. S. Bethune, R. M. Shelby, T. Mori, R. Scheffler, A. Speidel, M. Sherwood and A. C. Luntz, *J. Phys. Chem. Lett.*, 2012, **3**, 3043-3047.
19. S. H. Oh and L. F. Nazar, *Adv. Energy Mater.*, 2012, **2**, 903-910.
20. J.-L. Shui, N. K. Karan, M. Balasubramanian, S.-Y. Li and D.-J. Liu, *J. Am. Chem. Soc.*, 2012, **134**, 16654-16661.
21. Z. Jian, P. Liu, F. Li, P. He, X. Guo, M. Chen and H. Zhou, *Angew. Chem. In. Edit.*, 2014, **53**, 442-446.
22. E. Yilmaz, C. Yogi, K. Yamanaka, T. Ohta and H. R. Byon, *Nano Lett.*, 2013, **13**, 4679-4684.
23. P. Bhattacharya, E. N. Nasybulin, M. H. Engelhard, L. Kovarik, M. E. Bowden, X. S. Li, D. J. Gaspar, W. Xu and J. G. Zhang, *Adv. Funct. Mater.*, 2014, **24**, 7510-7519.
24. B. Sun, P. Munroe and G. Wang, *Sci. Rep.*, 2013, **3**, 2247.
25. B. Sun, X. Huang, S. Chen, P. Munroe and G. Wang, *Nano Lett.*, 2014, **14**, 3145-3152.
26. F. Li, D. M. Tang, Z. Jian, D. Liu, D. Golberg, A. Yamada and H. Zhou, *Adv. Mater.*, 2014, **26**, 4659-4664.
27. F. Li, D.-M. Tang, T. Zhang, K. Liao, P. He, D. Golberg, A. Yamada and H. Zhou, *Adv. Energy Mater.*, 2015, **5**, 1500294.
28. N. Ding, S. W. Chien, T. S. A. Hor, R. Lum, Y. Zong and Z. Liu, *J. Mater. Chem. A*, 2014, **2**, 12433-12441.
29. Y. Chen, F. Li, D.-M. Tang, Z. Jian, C. Liu, D. Golberg, A. Yamada and H. Zhou, *J. Mater. Chem. A*, 2013, **1**, 13076-13081.
30. J.-B. Park, J. Lee, C. S. Yoon and Y.-K. Sun, *Acs Appl. Mater. Inter.*, 2013, **5**, 13426-13431.

Table of Contents.

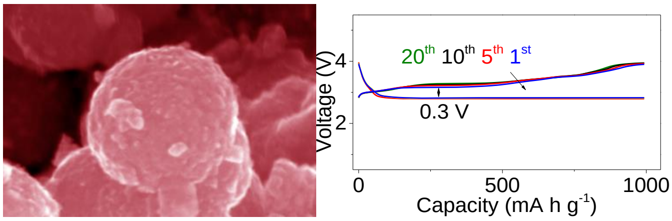

Carbon-free, hierarchical Ru nanospheres as a cathode for the Li-O_2 battery can significantly reduce discharge/charge overpotential with a high capacity.